Single-camera active stereo vision system using fiber bundles

Yexin Wang (王晔昕), Fuqiang Zhou (周富强)*, and Yi Cui (崔 毅)

Key Laboratory of Precision Opto-Mechatronics Technology, Ministry of Education, Beihang University, Beijing 100191, China

**Corresponding author: zfq@buaa.edu.cn*

Received April 7, 2014; accepted June 18, 2014; posted online September 18, 2014

We propose an approach for realizing 3D reconstruction in small field of view or some extreme environments. We combine the stereo vision and the structured light technologies and change the traditional ways of applying them by employing two fiber bundles. The processes of calibration and 3D reconstruction are also introduced. Experiments are performed to verify the feasibility and effectiveness of our proposed approach.

OCIS codes: 130.6010, 150.0155.
doi: 10.3788/COL201412.101301.

Currently, 3D vision reconstruction and measurement technologies cannot work properly in some extreme environments or small field of view (FOV) such as pipeline, engine, and boiler[1–3]. The difficulties are as follows: 1) bulky camera cannot be put into these "confined space" to capture images and 2) some of the extreme circumstances contain electromagnetic radiation or other damages that may destroy the imaging device. Therefore, a method that can conquer both these problems needs to be addressed.

Among all the 3D reconstruction technologies, stereo vision has the advantages of high accuracy, which is an effective way to realize 3D surface reconstruction, location and pose estimation, etc. Moreover, the use of catadioptric mirrors make stereo vision system more compact and low cost[4,5]. However, corresponding matching is a tough problem for some objects such as metal work piece and pipeline because there is no texture or extractable features. Although shape from shading can be applied to non-textured objects reconstruction[6], this technology requires complex surface reflectance model. Another way to enrich texture is to use structured light method. Generally, structured light uses laser generator or projector. Some researchers combined structured light with two cameras in order to provide extractable features[7]. But structured light with rich texture is usually generated by projector which is of large size to work in extreme environments aforementioned. None of the existing approaches concern both the stereo-structured-light combined method and the device flexibility for applications in small FOV and extreme environments.

We propose a compact, fiber bundles-based active stereo vision system, which combines catadioptric stereo technology and structured light. One fiber bundle is coupled to the projector on one end, and with an objective lens on the other end. This way, the fiber bundle transmits light generated by projector spreading them via an objective lens. Another fiber bundle is coupled to a camera on one end and with an objective lens and a pair of mirrors on the other end to form a stereo structure. The advantage of using fiber bundles as a means of transmitting light for optical imaging and projecting is that the camera and the projector can be placed away from the object, allowing the detector (i.e., the distal end) enter into extreme environments without damaging the camera and projector. According to this design, the detector can be attached to a mobile robot or other devices to implement more fields of applications such as 3D reconstruction based on mosaic images, navigation, and object tracking[8–10]. Figure 1 shows the setup of our active stereo vision system. The system is constructed by three sub-systems: 1) projection sub-system; 2) stereo imaging sub-system; 3) the detector. Figure 2 shows a detailed structure of the projection sub-system. A digital light processing (DLP) projector is controlled by a computer to generate stripes, dots, or any other features, and it is connected to a fiber bundle via a telecentric lens. As shown in Fig. 2, a stripe image, for example, is generated by the projector, and the light travels into the telecentric lens and gathers on one end of the fiber bundle. The image is reduced in size by the telecentric lens. Then the light

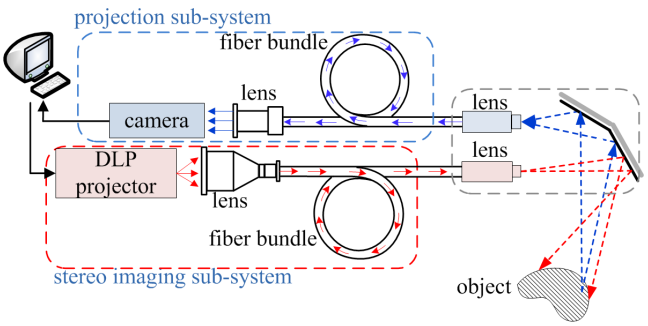

Fig. 1. Setup of our active stereo vision system.

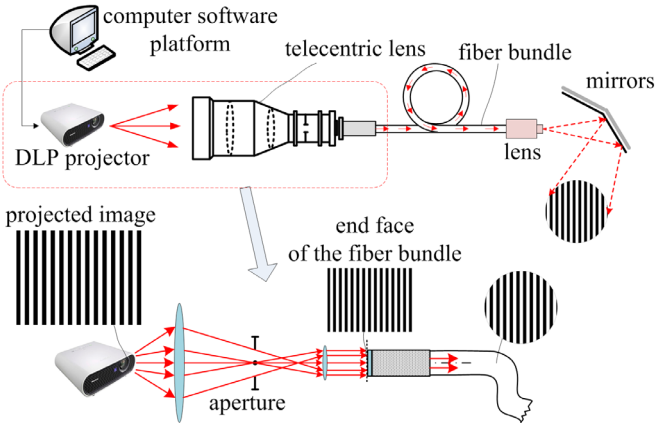

Fig. 2. Structure of the projection sub-system.

continues to travel and come out from the other end of the fiber bundle where an objective lens is coupled to it. Then the lens spreads the light onto one of the mirrors lighting the object surface. For details on the design and analysis of the telecentric lens one can refer to our previous work[11].

Figure 3 shows a detailed structure of the stereo imaging sub-system. Object reflects the light that is projected by the projection sub-system. In Fig. 3, red line represents the projected features. The light from the object travels to the mirrors in the detector, and gets reflected by the two mirrors into two different directions. An objective lens that is coupled to the end face of the fiber bundle absorbs the light and transmits it into the fiber bundle. On the other end of the fiber bundle, a telecentric lens is used for adjusting the images size to accord with the camera image size. The so-called stereo image is actually one image. Because a pair of mirrors is used, the camera's FOV is divided into two parts: the left and the right parts[5]. The measured object images on both parts of the image simultaneously.

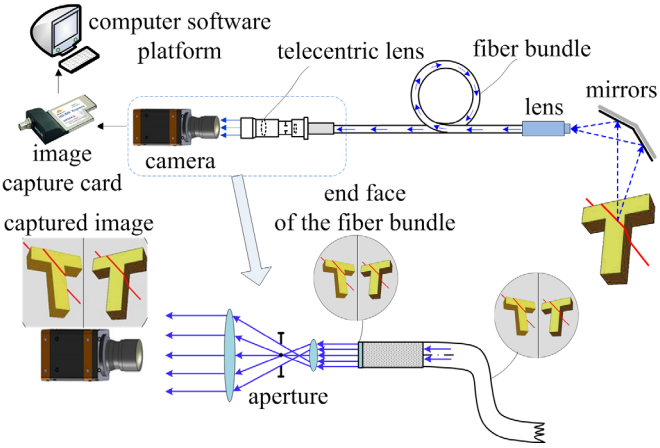

Fig. 3. Structure of the stereo imaging sub-system.

As fiber bundle has the advantages such as passive, anti-vibration, and insensitive to magnetic fields, which overcomes the disadvantages of traditional CCD or CMOS cameras used in these areas. Besides, fiber bundle is flexible, so it can reach some extreme environments, such as VIVO, pipeline, and boiler, to acquire images. However, a disadvantage of using fiber bundles for image transmission is that the resolution of the system is limited by the diameter and the spacing of the bundle's individual fibers, which would cause undersampling the object. Therefore, the system resolution is determined by the optical device that has the lowest resolution.

Figure 4(a) shows the design of the detector, and Fig. 4(b) shows the real one with its upper cover removed. The detector is like a distal end of an endoscope, which is much smaller than the telecentric lens, cameras, and computer. Thanks to the flexible fiber bundles, the detector can be put into some confined space or small space by adding driving or navigation mechanical device. The bulky devices can be put outside where the environment is safe for the camera and other equipments. The size of the detector is 46×26×29 (mm). The working distance of the detector is 5–15 cm. The resolution of the fiber bundle in the projection sub-system is 19,000, with the diameter of each fiber 15 μm. In the stereo imaging sub-system, the resolution of the fiber bundle is 30000, with the diameter of each fiber 0.8 μm. The objective lens' angle of view is 55°, and the working distance is 10–40 mm.

Calibration task is crucial to the system, which is the prior step before 3D reconstruction and measurement[12]. As the projector is only for enriching the features on an object with no obvious texture, it does not need to be calibrated. Therefore, the calibration task only concerns determining the intrinsic parameters of the stereo imaging system such as focal length (f_x, f_y), principle point location (u_0, v_0), and lens distortions (k_1, k_2 for radial distortion, p_1, p_2 for tangential distortion), and the structure parameters such as rotation (3×3 matrix $\mathbf{R}$) and translation (3×1 vector $\mathbf{T}$) relations between the two virtual imaging system caused by the mirrors. For simplicity, we will call them the two virtual cameras in the following.

We used a calibration approach based on our previous work[13]. Assume the two virtual cameras share the same intrinsic parameters. First, a linear approximation

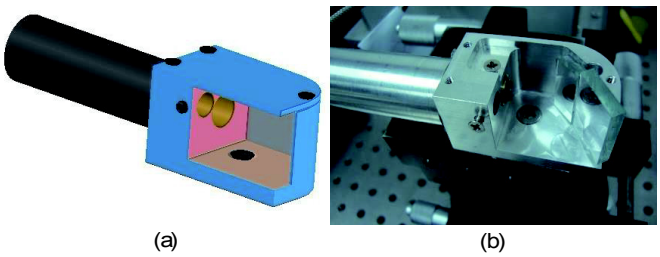

Fig. 4. (a) Design and (b) realization of the detector.

Table 1. System Parameters Obtained by Calibration

Parameter	f_x, f_y **(pixel)**	u_0, v_0 **(pixel)**	k_1, k_2 p_1, p_2	**R**	**T**
Value	1411.841	336.885	−0.238, −1.905	0.951, 0.00262, 0.308,	−6.150,
	1411.202	298.665	−0.000758, −0.00419	−0.00636, 1.000, 0.0111,	−0.211,
				−0.308, −0.0125, 0.951	1.394

aims at obtaining an initial guess of intrinsic parameters and structure parameters is used by establishing the correspondence of the known features locations in space and their extracted locations on the image. Then a further iterative algorithm is used to optimize the parameters so that the final parameters can be obtained, for more details please refer to Ref. [13]. We use a 2×2 dot pattern. The fabrication accuracy of the pattern here refers to the location accuracy of the dots which is ± 0.001 mm. The system parameters obtained by calibration using 20 captured images are listed in Table 1. The total RMS error is 0.128 pixel.

After calibration, we use our system to test 3D reconstruction of a metal object with curved surface. A captured image of the metal object is shown in Fig. 5(a). When there is only uniform lighting, it is hard to distinguish the shape (Fig. 5(a)). Here we use a stripe image to project on the metal object (Fig. 5(b)). The steps to match corresponding points are as follows: 1) get the image coordinates of the light stripes at the center using method described in Ref. [14]. 2) Calculate the epipolar line on the right half of the image for every extracted point on the left half of the image. 3) The corresponding point candidate of the left point is selected by a threshold which is the distance from the feature points on the right half to the epipolar line. 4) Use the candidate to repeat the process in the other way (i.e., from right to the left halves of the image). If the distance is also smaller than the threshold, these two points can be considered matched successfully. Here we set the threshold to be 0.01 pixel. Finally, triangulation can be accomplished to obtain the 3D coordinates of the matched points (Fig. 5(c)). Figure 5(d) shows its 3D reconstruction result that excluded the outliers.

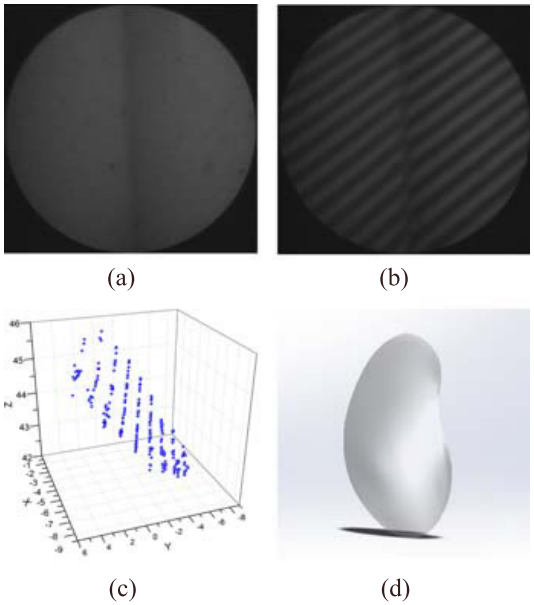

Fig. 5. 3D reconstruction experiment: (a) part of a cylinder-shaped work piece, (b) Projected stripes on the work piece, (c) point cloud of the matched corresponding points (unit: mm), and (d) 3D reconstruction result.

In conclusion, we present an active stereo vision system for small FOV applications. In this system, a structured light technology using projector is applied to small FOV by adopting a fiber bundle to reduce the projected image size. In addition, a stereo vision structure is constructed using a pair of mirrors and is also applied in small FOV by employing another fiber bundle. The use of projection solves matching problem for non-featured objects. Moreover, the use of fiber bundles adds flexibility to the system so that the detector can be put into extreme environments without worrying about the damage possibility of the camera and computer. We describe the process of obtaining 3D information. The experimental results show that the active stereo vision system is of good accuracy and effective, which is a potential way of acquiring 3D information in small FOV or in extreme environment.

This work was supported by the National Natural Science Foundation of China (No. 60972086) and the Research Fund for the Doctoral Program of Higher Education of China (No. 20101102110033).

References

1. V. D. Sars, S. Haliyo, and J. Szewczyk, Mechatronics **20**, 251 (2010).
2. P. G. Papageorgas, D. Maroulis, G. Anagnostopoulos, H. Albrecht, B. Wagner, D. K. Iakovidis, and N. G. Theofanous, IEEE Trans. Instrum. Meas. **55**, 1725 (2006).
3. A. Landstrom, M. J. Thurley, and H. Jonsson, in *Proceedings of DICTA* 1 (2013).
4. G. Jang, S. Kim, and I. Kweon, Opt. Lett. **31**, 41 (2006).
5. J. Gluckman, and S. K. Nayar, Int. J. Comput. Vis. **66**, 65C79 (2001).
6. V. S. Ramachandran, Nature **331**, 163 (1988).

7. F. Bruno, G. Bianco, M. Muzzupappa, S. Barone and A. V. Razionale. ISPRS J. Photogramm. Remote Sensing **66**, 508 (2011).
8. H. Wang, Y. H. Liu, W. Chen, and Z. Wang, IEEE/ASME Trans. Mechatron. **16**, 387 (2011).
9. N. Gans, G. Hu, K. Nagarajan, and W. E. Dixon, IEEE Trans. Robot. **27**, 822 (2011).
10. R. Liu and Z. Jing, Chin. Opt. Lett. **10**, 021001 (2012).
11. F. Wang and F. Q. Zhou, Electro-Opt. Technol. Appl. **6**, 32 (2007).
12. F. Zhou, Y. Wang, Y. Cui, and H. Tan, Chin. Opt. Lett. **10,** 021003 (2012).
13. F. Q. Zhou, Y. X. Wang, B. Peng, and Y. Cui, Measurement **46**, 1147-C1160 (2013).
14. C. Steger, IEEE Trans. Pattern Anal. Mach. Intell. **20**, 113-C25 (1998).